

Temperature effects on dislocation core energies in silicon and germanium

Caetano R. Miranda

*Instituto de Física “Gleb Wataghin”, Universidade Estadual de Campinas,
CP 6165, CEP 13083-970, Campinas, SP, Brazil*

R. W. Nunes

*Departamento de Física, Universidade Federal de Minas Gerais,
Belo Horizonte, Minas Gerais , CEP 30123-970, Brazil*

A. Antonelli

*Instituto de Física “Gleb Wataghin”, Universidade Estadual de Campinas,
CP 6165, CEP 13083-970, Campinas, SP, Brazil*

(November 19, 2018)

Abstract

Temperature effects on the energetics of the 90° partial dislocation in silicon and germanium are investigated, using non-equilibrium methods to estimate free energies, coupled with Monte Carlo simulations. Atomic interactions are described by Tersoff and EDIP interatomic potentials. Our results indicate that the vibrational entropy has the effect of increasing the difference in free energy between the two possible reconstructions of the 90° partial, namely, the single-period and the double-period geometries. This effect further increases the energetic stability of the double-period reconstruction at high temperatures. The results also indicate that anharmonic effects may

play an important role in determining the structural properties of these defects in the high-temperature regime.

I. INTRODUCTION

The study of the atomic structure of dislocation cores in semiconductors is not free from outstanding issues.¹⁻⁴ At low deformations, dislocations in these systems are known to occur along $\langle 110 \rangle$ directions on $\{111\}$ slip planes of the diamond (or zinc-blend) lattice. Due to the presence of a two-atom basis, this lattice supports two possible $\{111\}$ dislocation slip planes, the so-called glide and shuffle sets. In the glide set, the slip plane lies between atomic layers separated by a third of the nearest-neighbor bond length, and geometrically it would appear that dislocation glide should require breaking three covalent bonds. In the case of the shuffle set, the slip plane lies between atomic layers separated by a full bond length, and glide appears to involve breaking only a single covalent bond. This would suggest that lattice friction should be smaller in the shuffle set, and hence that dislocations would glide in that configuration. However, the prevalent opinion is in favor of the glide set, based primarily on the experimental evidence showing that dislocations in Si are dissociated into Shockley partials bounding stacking-fault ribbons, and on the fact that stacking faults are not stable in the shuffle plane.¹⁻⁴ Nevertheless, this conclusion has been disputed by Louchet and Thibault-Desseaux,⁵ who argued that partials in the shuffle position could occur in conjunction with glide-plane stacking faults. The mechanism controlling dislocation glide is also a matter of debate. Many theoretical and experimental works have either supported or assumed the Hirth and Lothe mechanism,⁶ based on kink nucleation and migration, but an impurity-pinning mechanism proposed by Celli et al.⁷ has been shown to be consistent with recent experimental results.⁸ This issue is far from being resolved.

Another unresolved issue has recently arisen, regarding the core structure of the 90° partial dislocation. In $\{111\}$ planes, dislocations lining along $\langle 110 \rangle$ directions have their Burgers vectors either parallel (the screw orientation) or making a 60° angle with the dislocation line. Both dissociate into Shockley partials, the former into two 30° partials, and the latter into a 30° partial and a 90° partial. Both partials are believed to undergo core reconstruction, as indicated by the low density of unpaired spins found in EPR experiments.¹⁻⁴

In the glide set, the nature of the reconstruction of the 90° partial appears straightforward. The symmetrically-reconstructed geometry shown in Fig. 1(a) displays mirror symmetries along the $[110]$ direction. A symmetry-breaking reconstruction shown in Fig. 1(b) lowers the core energy by ~ 200 meV/Å, according to *ab initio* and tight-binding (TB) calculations.^{9–11} This structure retains the periodicity of the lattice along the dislocation direction, thus being called the single-period (SP) structure. Until recently, it had been a matter of consensus that the SP core was the “ground-state” structure of the 90° partial, since the earliest independent works of Hirsch and Jones.^{12,13} However, the structure shown in Fig. 1(c) has been recently proposed by Bennetto and collaborators,¹⁴ and shown to have lower internal energy than the SP core, by means of total-energy tight-binding (TETB), and *ab initio* local-density-approximation (LDA) calculations. In this new geometry, along with the mirror symmetry, the translational symmetry of the lattice by a single period is also broken, and the periodicity along the core is doubled. For that reason, this reconstruction has been called the double-period (DP) structure.

Both the SP and DP geometries are consistent with all available experimental information about the 90° partial. EPR measurements in Si indicate a rather small density of dangling bonds in the core of the dislocation.^{1–3} The two structures are fully reconstructed, meaning that neither would give rise to deep-gap states which would show an EPR signal. Moreover, both cores consist entirely of fivefold, sixfold, and sevenfold rings, both being consistent with images produced by transmission electron microscopy, at the current level of resolution of this technique.⁸ So far, the experiments appear unable to decide clearly on the issue. Recent experimental work by Batson¹⁵ indicates a DP-derived structure (called the “Extended DP structure” by this author) to be more consistent with STEM and EELS experiments.

At the theoretical level, several calculations have addressed the energetics of the SP and DP cores in diamond (C), silicon (Si), and germanium (Ge), using different methods.^{14,16–21} Virtually all of the more accurate *ab initio* and TETB studies^{14,17–20} agree that the DP core is more stable at 0 K, with the exception of the *ab initio* cluster calculations for Si in Ref. 21. For example, LDA and TETB calculations in Refs. 14 and 20 indicate that the

internal energy of the DP structure is lower than that of the SP core in all three materials (C, Si, and Ge). A possible influence of supercell boundary conditions on these results was raised in Ref. 21 (using Keating-potential calculations) and later refuted by supercell-size converged TETB calculations in Ref. 17. The issue was further revisited in Ref. 18, with *ab initio* calculations showing that the DP core remains more stable in C even under relatively severe stress regimes. Ideally, supercell-size converged calculations like the TETB ones in Ref. 17 would properly address the issue for isolated dislocations in the bulk. However, in that study very large supercells (containing up to 1920 atoms) were employed, which makes such calculations prohibitive for the more accurate *ab initio* techniques.

Closely related to the present study is the work of Valladares and co-workers,¹⁶ in which temperature effects on the energetics of the SP and DP cores in Si were investigated using a Tersoff potential,²² within a harmonic approximation treatment of vibrational entropic effects in the dislocation free energy, at finite temperatures. They find that the free-energy difference between the two cores, at a temperature of 800 K, becomes smaller than the zero-temperature internal energy split, suggesting the possibility of the two cores playing a role in the plasticity of Si, in the temperature range of most plastic deformation experiments (~ 700 - 1000 K). However, the calculations in Ref. 16 did not include anharmonic effects, which are likely to be relevant in that range of temperatures.

In this paper, we present the results of a study of anharmonic vibrational effects in the free-energy difference between the SP and DP cores in Si and Ge. As discussed in the following, we arrive at different conclusions with respect to the work of Valladares *et al.*, with our results indicating that the effect of increasing temperature is to enhance the thermodynamical stability of the DP core with respect to the SP geometry. In our calculations, anharmonic effects are fully taken into account by using a methodology that allows to estimate the free energy through non-equilibrium simulations. The details of this methodology are discussed in Sec. II. In Sec. III our results are presented and discussed. We end with a summary and conclusions in Sec. IV.

II. METHODOLOGY

A. Interatomic Potentials

There are several empirical potentials available in the literature to model the interactions between Si atoms.²³ In the present work, our aim is to account for vibrational entropic effects on the energetics of the SP and DP reconstructions of the 90° partial dislocation in Si. One key ingredient for this purpose is that both the SP and DP structures be a local minimum of the potential. It is essential then that the potential be able to describe the reconstruction-driven symmetry breaking that leads to the SP geometry.^{9–11} This is an important aspect, since both core structures consist of fully reconstructed bonds, and a realistic description of vibrational properties requires a proper treatment of bonding for the minima in question. For example, potentials such as the Stillinger-Weber(SW) and the Kaxiras-Pandey(KP) fail in that regard.²⁴ Both the Tersoff²² and the Environment Dependent Interatomic Potential (EDIP)^{25,26} models describe correctly the energetics of the SP reconstruction with respect to a symmetric (so-called quasi-fivefold) structure.^{9,26}

The focus of our paper is on the effects of the dislocation vibrational modes on the free energies of the two core models at finite temperatures. In a previous work we have used these two potentials to estimate the free energy of Si in several different phases (amorphous, liquid, and crystalline, as well as clathrate structures), obtaining results which are in good agreement with those of experimental and other theoretical works.²⁷ For a more specific analysis of the description of anharmonic effects by the EDIP and Tersoff potentials, we show in Fig. 2 the results we obtained for the free energy as a function of temperature, in a 216-atom bulk supercell. The figure includes also the Tersoff-potential harmonic approximation values from Ref. 28 and the experimental results from Ref. 29. As expected, the experimental numbers start deviating appreciably from the harmonic approximation curve around the Debye temperature of Si (~ 640 K), where anharmonic effects begin manifesting themselves. From the figure, we see that both the Tersoff and the EDIP potentials can account for these

anharmonic effects in the free-energy curve at a quantitative level.

Moreover, it is clear that the EDIP results are in better agreement with the experimental ones. Of particular relevance to the present work is the scale of the difference in free energy between harmonic-approximation and experimental results, which is ~ 10 meV/atom at 640 K. As a first approximation, we may consider ten atoms per period as constituting the core in the SP and DP structures (those taking part in the fivefold and sevenfold rings, seen on [110] projections, surrounding the geometric center of the core), which gives an initial estimate of ~ 30 meV/Å for the scale of the anharmonic effects, from the bulk results. From this, one might expect that anharmonic effects should be important in the case of the 90° partial, since the difference in enthalpy at 0 K between the SP and DP cores is ~ 60 meV/Å.

On the basis of these results, we argue that both potentials give a realistic description of vibrational effects, in particular of the anharmonic contributions which become important in the range of temperatures of our study. For the Ge case, only a Tersoff model was employed, since there are no available parameters for Ge in the EDIP form. The functional form and the parameters we use for the two models are given in Refs. 22 (Tersoff) and 26 (EDIP).

B. Simulations and Free Energy Calculations

In our statistical computation of dislocation free energies, we use a Metropolis-algorithm Monte-Carlo method. Two types of simulations were performed, one employed a canonical-ensemble (constant-NVT) treatment, and the other simulated an isobaric-isothermal ensemble (constant-NPT).³⁰ A simulation cell with 192 atoms was used, containing a 90° partial-dislocation dipole which was introduced by displacing the atoms according to the continuous-elasticity solution for the displacement field of a dislocation dipole.⁶ The introduction of a dipole enables the use of periodic boundary conditions to avoid surface effects. It should be pointed out that the free energy calculations presented in this work are far more demanding in terms of computer time than harmonic-approximation calculations, which only require one diagonalization of the dynamical matrix, in order to determine the phonon fre-

quencies. Therefore, the complexity of our calculations imposes a limitation on the size of the cell used in the simulations. The cell size chosen reflects the best compromise between a good description of the essential physics and computational feasibility.

The free energy calculations were performed using a non-equilibrium method, namely the Reversible-Scaling method (RS).³¹ This method consists of simulating a quasi-static process where the potential-energy function of the system is dynamically scaled. It allows for an accurate and efficient evaluation of the free energy over a wide range of temperatures, using a single Monte Carlo simulation, starting from a reference temperature for which the free energy of the system is known. In order to obtain the free energy at this reference temperature, we used the Adiabatic Switching method (AS).³² Using the AS approach, the absolute free energy can be computed by determining the work done to switch the potential energy of the system from the configuration of interest to that of a reference system for which the free energy is known analytically. The systematic error in the free energy, caused by dissipation, can be estimated by reversing the switching procedure and computing the overall work performed in this round-trip procedure. The statistical error can be estimated by performing several trajectories in the configuration space of the system.

In this work, the reference system was an Einstein crystal, i.e., a collection of independent harmonic oscillators. The angular frequency of the oscillators (ω) was taken to be approximately the vibration modes of Si ($\omega = 28$ Trad/s) and Ge ($\omega = 15$ Trad/s), which correspond to the acoustic phonon modes from the edge of the Brillouin zone that give rise to a pronounced peak in the phonon density of states of these materials.^{33,34} It should be pointed out that the final value for the Gibbs free energy is not sensitive to the choice of the oscillator frequency, provided that the chosen frequency is not very far from the relevant frequencies of the physical system. Monte Carlo constant-NVT simulations were used to generate switching trajectories, with a typical "switching time" of 3.0×10^5 MC/steps. The volume in these simulations was chosen to be that obtained from a constant-NPT simulation for the given reference temperature at zero pressure. In general, 25 switching trajectories were used to estimate the statistical error. The estimated error was $\pm 1.0 \times 10^{-3}$ eV/atom.

RS calculations were carried out at zero pressure, covering a range from $T=100$ K to $T=2000$ K, using a scaling time of 5.0×10^5 MC/steps. Five different switching trajectories were sampled, in order to estimate the statistical errors. In this way, we were able to estimate the absolute Gibbs free energy (G_{abs}) at zero pressure of the SP and the DP reconstructions in the interval from 300K to 1200 K using EDIP and Tersoff models for Si, and for Ge in the same range of temperatures using a Tersoff potential. The absolute vibrational entropy was calculated by taking the numerical derivative of the absolute Gibbs free energy with respect to temperature: $S_{abs} = -(\frac{\partial G_{abs}}{\partial T})$.

III. RESULTS AND DISCUSSION

A. Enthalpies at zero Kelvin

Imposing periodic boundary conditions in a dislocation calculation using supercells requires the net Burgers vector in the cell to vanish. This is done by using cells which contain two dislocations with opposite Burgers vectors. Hence, besides the core enthalpies that interest us, supercell calculations also include elastic interactions between the two dislocations, and between the dislocations and their periodic images. In order to extract meaningful core energy values, these elastic interactions must be properly accounted for. Previous calculations have shown that dislocation cores in covalent semiconductors are very narrow, with the elastic fields reaching the linear behavior predicted by the continuum linear elasticity solution already at a distance of about two lattice periods from the center of the core.^{11,18} This indicates that, to the extent that one is interested in differences in energies between different core models, long-range elastic effects should mostly cancel out for sufficiently large cells. This is because these long-range fields are defined by the dislocation slip system which is obviously the same in our case, since we are comparing different core structures of the same dislocation. We must be careful, however, in providing numerical evidence that the supercells we use in our calculations are sufficiently large, in the above sense.

In the particular case of the SP geometry, it is known that a relatively strong dipolar elastic interaction is present, which depends on the relative senses of reconstruction of the two dislocations in the cell, with respect to the broken mirror symmetry. Depending on the size of the cell, this interaction may be of the same order of the core-energy difference between the SP and DP geometries. (A similar effect is present in the DP core, but this is a weaker quadrupolar interaction which can be neglected.¹⁴) As discussed in the literature,^{14,16–20} this dipolar interaction can be properly handled by considering the SP-core energy as the average energy between two supercell calculations, one in which the two SP dislocations are reconstructed in the same sense, and the other where they have opposite reconstruction senses.^{17,19,20} In order to further investigate the accuracy of this procedure and also to address the numerical convergence level of our calculations for the cell sizes we use, we show in Table I the 0 K enthalpies computed with the Tersoff and EDIP potentials for several different cell sizes. For comparison, we also include the TETB results from Ref. 17, to which we add numbers for a 240-atom supercell. In the notation introduced in Ref. 21, the relevant supercell parameters are D , the height of the cell in the $\langle 111 \rangle$ direction (perpendicular to the slip plane), and L the width of the cell in the $\langle 11\bar{2} \rangle$ direction (perpendicular to the dislocation line) on the slip plane. We consider here only supercells with “dipolar” boundary conditions,³⁵ which were shown by Lehto and Öberg²¹ to minimize the strains associated with the stacking of the infinite array of dislocations. We will comment below on the comparison of our results with those from Ref. 16, which were obtained with “quadrupolar” boundary conditions.³⁵

Table I shows our results for $E_{SP-DP} = \bar{E}_{SP} - E_{DP}$, the energy difference between the average energy of the two SP cells (\bar{E}_{SP}) and the energy of the DP cell, and for $\Delta E_{SP} = E_{SP}^{same} - E_{SP}^{opposite}$, the energy splitting between the two SP cells (as described in the previous paragraph), for four different cell sizes. Note that E_{SP-DP} converges for relatively small cell sizes, and faster than ΔE_{SP} , due to the cancellation of elastic effects that happens when we take the average of the two SP calculations. For the free-energy calculations we discuss in the next section, we used the smaller cell, with $L = 13.3 \text{ \AA}$ and $D = 18.8 \text{ \AA}$, for a total of

192 atoms. In the 240 atom cell, D is the same as in the 192-atom cell, and L is only 25% larger. We can see from Table I that, already for this 240-atom cell, the TETB result for E_{SP-DP} is converged to within the numerical accuracy of the method. This is also what can be observed for the EDIP potential. The EDIP result for E_{SP-DP} in the 192-atom cell is within 13% of the EDIP converged value, and for the 240-atom cell E_{SP-DP} is converged to within 3%. The Tersoff numbers converge more slowly, with the 192-atom cell numbers being more than twice as large as the converged value. In the case of Ge, we only calculated E_{SP-DP} using the 192-atom cell. We obtained $E_{SP-DP} = -8 \text{ meV}/\text{\AA}$ in disagreement with the LDA and Keating-potential results from Ref. 19. However, as discussed in Sec. III B, the behavior of the free energy as a function of temperature for Ge is the same as that for Si, i.e., E_{SP-DP} increases as the temperature is raised. If we were to extrapolate to the free-energy calculations these convergence trends observed for the 0 K enthalpy results in Table I, we would expect our EDIP free-energy values to be converged to within $\sim 10\%$, and the Tersoff values to be about twice as large as what we would obtain with larger cells.

The TETB calculations in Table I were done at the fixed cell volume (corresponding to the experimental lattice constant). As a test, we also performed calculations for volumes 1% larger and smaller, obtaining the same convergence trends, i.e., energies were essentially converged for the 240-atom cell. More importantly, the convergence calculations with the Tersoff and EDIP potentials in Table I were done at constant pressure, resulting in very small changes from the initial volumes.

Before proceeding to the discussion of the free-energy results, let us put the results in Table I in perspective. Previous studies have shown that the Tersoff potential does give the right ordering of 0 K enthalpies, despite underestimating the difference in enthalpies between the two cores. Our converged Tersoff values of $6 \text{ meV}/\text{\AA}$ are in very good agreement with the converged results obtained in Ref. 36 using supercell and cylindrical cluster calculations. However, they are smaller by one order of magnitude, when compared with the converged TETB values. The EDIP potential has the shortcoming of predicting the wrong ordering of 0 K enthalpies for the SP and DP cores. When comparing our results with those obtained

by Valladares *et al.*, we must observe that they used cells with $D = 9.4 \text{ \AA}$, which is half the height of our cells, and quadrupole boundary conditions. As a check, we did run Tersoff calculations with the same cell parameters and obtained the same results as in their work. The value for E_{SP-DP} in this case is 32 meV/\AA , which is more than five times as large as the converged Tersoff value in Table I. This shows that, at least for the 0 K enthalpy, their results are not converged at the same level as our calculations.

B. Free energies

In order to test whether the empirical potentials support the SP and DP reconstructions at high temperatures, we performed constant-NPT simulations of all structures in a broad range of temperatures, from 0 K up to 2000 K (1500 K) for Si (Ge). The structures were further characterized for several temperatures (at every 500 K between 0 K and the highest temperature) by evaluating structural properties such as the pair-correlation function, the bond-angle distribution, and the atomic-coordination number. Only the natural thermal broadening of these functions was observed, with no structural changes and all atoms remaining fourfold coordinated. From these results, we conclude that for both the Tersoff and the EDIP potentials, the SP and DP reconstructions remain stable and do not undergo restructuring over the entire range of temperatures we tested for each of the two semiconductors.

The metastability of the SP core, even at temperatures as high as 2000 K, is not surprising. Unlike the spontaneous transformation of the symmetric quasi-fivefold core into the SP core, which happens at 0 K due to the absence of an energy barrier,⁹⁻¹¹ the SP \rightarrow DP transformation involves breaking the strong reconstructed covalent bonds in the SP core. The same bond breaking mechanism regulates the kink migration barriers.¹⁰ We have computed an energy barrier of $\sim 1.5 \text{ eV}$ for the process involving the conversion of a segment of two SP periods into a segment of one DP double period.

Let us now turn to the focus of this work, the Gibbs free-energy difference, ΔG , between

the SP and the DP cores as a function of temperature, obtained by the Reversible Scaling Method within the Monte Carlo method (RS-MC). In the previous section we discussed the numerical convergence of our calculations with respect to the two dimensions of the supercell which are perpendicular to the dislocation line. When we introduce thermal effects, periodicity along the line is disrupted by atomic vibrations, and one must be careful about the sampling of the phonon modes along the dislocation direction. In our free-energy calculations, we used 192-atom supercells with twice the lattice period along this direction. To test the phonon sampling in this cell, we also calculated free energies for a supercell with four times the lattice period along the line, using the Tersoff potential. In Fig. 3 we show the results for the free-energy difference ΔG between the SP and DP cores, for the two types of SP cells and also for the average between the two cells. Note that, while the results for ΔG for the individual SP calculations differ quite appreciably for a given cell size and vary substantially when we go from the smaller (192 atoms and twice the lattice period along the dislocation line) to the larger cell (384 atoms and four times the period along the line), the results for ΔG between the average of the SP cells and the DP cell are very similar for the two cell sizes. This shows that our simulations with 192 atoms capture most of the relevant differences between the vibrational modes of the two cores and also lends further confirmation of the cancellation of elastic interaction effects that occurs when the average between the two SP cells is considered, as discussed in the previous section.

In Fig. 4 we show the results for ΔG_{SP-DP} for the Tersoff and EDIP models in a 192-atom supercell, showing now only the average of the SP calculations. Fig. 5 shows the results for Ge using the Tersoff potential. In order to analyze the entropic effects, Figs. 4 and 5 also display the entropic contribution ($-T\Delta S$) to ΔG . The Tersoff results for Si in Fig. 4 show ΔG increasing with temperature from 19 meV/Å at 300 K to 37 meV/Å at 1200 K. The entropic term also increases with temperature, being the dominant contribution for ΔG in the high temperature regime. For Si using the EDIP model, we observe the same behavior, with ΔG increasing with temperature from -32 meV/Å at 300 K to -23 meV/Å at 1200 K, notwithstanding the fact that for this potential the SP core remains more stable

over the entire temperature range. This is mostly due to the fact that the EDIP potential does not describe properly the energetics of the two reconstructions at 0 K, as discussed above. But even for this potential, the behavior of the entropic term is determinant of the temperature trend observed for ΔG , which is qualitatively the same trend observed with the Tersoff model. As indicated by the convergence trends we discussed in the previous section for the 0 K enthalpies, a quantitative comparison between the changes in ΔG produced by the Tersoff and EDIP potentials would suffer from the fact that, for the 192-atom cell, the Tersoff results could be overestimated by as much as a factor of two. Note that, for silicon, the overall change in ΔG over the 300 K - 1200 K interval is 18 meV/Å for Tersoff and 9 meV/Å for EDIP. While speculative, it seems reasonable to expect that the overall change in ΔG for the two potentials, over the temperature range of our calculations, would be in good agreement if we used cells with larger values of D and L .

Regarding the contribution of the entropic term depicted in Figs. 4 and 5, two points have to be emphasized. First of all, the entropy is calculated by taking the numerical derivative of the free energy, and the numerical data for this quantity presents some statistical fluctuations. Most certainly, these fluctuations are bound to be enhanced when one takes numerical derivatives. This explains some of the oscillations observed in the entropic term. Thus the qualitative behavior of the total free-energy is more representative than the behavior of the isolated entropic term shown in the figures. Another point has to do with the behavior of the entropic term as a function of temperature, in particular for the computations using the Tersoff potential. The free energy difference ΔG is quite small, when compared with the total free energy of each system, and the same is true for the entropic contribution to this difference. These energy differences will be affected by anharmonic effects, and the discrepancy between the entropic term computed using the two models (EDIP and Tersoff) above 600 K is related to the way anharmonic effects are accounted for in each model. It is clear from Fig. 2 that the results obtained using the Tersoff potential tend to deviate more from the experimental data than those obtained using the EDIP, and that the difference between the two potentials increase with increasing temperature. The more accentuated increase

in the entropic term computed using the Tersoff potential has to do with its tendency to overestimate the anharmonic effects, and represents a small amount of energy that is not related to any changes in the structure of the defect (which would imply in much bigger changes in the free energy).

In the case of Ge, ΔG increases with temperature faster than in Si (compared to either of the Si potentials used), from 2 meV/Å at 300 K to 33 meV/Å at 1200 K. While the enthalpy difference at 0 K marginally favors the SP reconstruction (at variance with the LDA result in Ref. 20), the behavior of the free energy suggests that at room temperature the DP reconstruction would be more stable than the SP structure. It is important to emphasize the similarity between our results for Si and Ge, i.e., the free energy difference ΔG increases with temperature in both cases (the increase rate is larger in Ge than in Si), meaning that the entropic term leads to an enhancement of the thermodynamical stability of the DP structure with respect to the SP, as the temperature increases.

At this point it is interesting to compare the RS-MC results for Si with the harmonic-approximation calculations of Valladares *et al.*¹⁶ In Fig. 6, we show our RS-MC calculations using the Tersoff (full line) and EDIP (dashed line) models, and the Tersoff harmonic-approximation results from Ref. 16 (dotted line). For a better comparison of the temperature trends in each calculation, our values for ΔG for both potentials have been shifted such that they extrapolate to the same zero-temperature ΔG value obtained by Valladares *et al.* The same qualitative behavior is observed in Fig. 6 for the RS-MC calculations using both the Tersoff and the EDIP models. In both cases, ΔG *increases* with temperature, while the opposite is observed for the harmonic-approximation calculations, which show ΔG *decreasing* with increasing temperature. This points to an important role of anharmonic effects in describing thermal effects on dislocation cores in semiconductors.

It should also be pointed out that at low temperatures our results cannot be directly compared to those in Ref. 16, because their calculations take into account quantum effects which are absent in our approach. While quantum effects may be relevant at low temperatures, we are mostly concerned with the anharmonic effects, which become more relevant in

the high-temperature regime. Valladares *et al.* point out that the order of magnitude of the difference in free energies between the SP and the DP reconstructions is smaller than the thermal energy ($k_B T$) over the entire range of temperature in their study. This would suggest that the two structures would be nearly equally stable. Our results, however, indicate that at high temperatures the free energy difference between the SP and the DP cores is of the same order of the thermal energy. Therefore, considering that the thermal fluctuations are smaller than the thermal energy itself, our results suggest that the DP reconstruction should be dominant in the high temperature regime. In other words, while thermal fluctuations may account for the creation of local defects such as kinks, it is unlikely that these fluctuations may cause substantial portions of the dislocation to switch from the DP to the SP reconstruction (barring a possible dependence of the core energies on the stress acting on the dislocation,¹⁸ an issue that has not yet been investigated in Si and Ge).

IV. CONCLUSIONS

In this work, we studied the differences in free energies and vibrational entropies between the SP and DP core reconstructions of the 90° partial dislocation as a function of temperature in silicon and germanium, using a Reversible Scaling Method and Monte Carlo simulations, with Tersoff and EDIP models for the energetics. This methodology is a fully-classical simulation which includes all anharmonic vibrational effects. Our results indicate that the difference in the free energies (and in the vibrational-entropy contribution to this quantity) between the two core structures increases with temperature in both materials. In the case of Si, this behavior occurs for both potentials used in the calculations. This is in contrast with the free-energy calculations by Valladares and co-workers¹⁶ which incorporates vibrational-entropy effects only at the harmonic-approximation level. Our calculations indicate that the DP reconstruction, which is lower in energy at 0 K, becomes even more stable with respect to the SP structure in the high temperature regime. Moreover, our results also suggest that the anharmonic effects may play an important role in the description of the thermal behavior

of extended defects in semiconductors.

ACKNOWLEDGMENTS

C. R. Miranda and A. Antonelli acknowledge the support from the Brazilian funding agencies: FAPESP, CNPq, and FAEP. R. W. Nunes acknowledges support from the Brazilian agencies: CNPq and FAPEMIG.

REFERENCES

- ¹ P. B. Hirsch, *Mater. Sci. Tech.* **1**, 666 (1985).
- ² M. S. Duesbery and G. Y. Richardson, *Crit. Rev. Solid State Mater. Sci.* **17**, 1 (1991).
- ³ H. Alexander and H. Teichler, in *Materials Science and Technology*, edited by R. W. Cahn, P. Hassen, and E. J. Kramer (VCH Weinheim, Cambridge, 1993), Vol. 4, p. 249.
- ⁴ V. V. Bulatov, J. F. Justo, W. Cai, S. Yip, A. S. Argon, T. Lenosky, M. de Koning, and T. Diaz de la Rubia, *Philos. Mag. A* **81**, 1257 (2001).
- ⁵ F. Louchet and J. Thibault-Desseaux, *Rev. Phys. Appl.* **22**, 207 (1987).
- ⁶ J. P. Hirth and J. Lothe, *Theory of Dislocations* (Wiley, New York, 1982).
- ⁷ V. Celli, M. Kabler, T. Ninomiya, and R. Thomson, *Phys. Rev.* **131**, 58 (1963).
- ⁸ H. R. Kolar, J. C. H. Spence, and H. Alexander, *Phys. Rev. Lett.* **77**, 4031 (1996).
- ⁹ J. R. K. Bigger, D. A. McInnes, A. P. Sutton, M. C. Payne, I. Stich, R. D. King-Smith, D. M. Bird, and L. J. Clarke, *Phys. Rev. Lett* **69**, 2224 (1992).
- ¹⁰ R. W. Nunes, J. Bennetto, and David Vanderbilt, *Phys. Rev. Lett* **77**, 1516 (1996).
- ¹¹ L. B. Hansen, K. Stokbro, B. I. Lundqvist, K. W. Jacobsen, and D. M. Deaven, *Phys. Rev. Lett* **75**, 4444 (1995).
- ¹² P. B. Hirsch, *J. Phys. (Paris), Colloq.* **40**, C6-27 (1979).
- ¹³ R. Jones, *J. Phys. (Paris), Colloq.* **40**, C6-33 (1979).
- ¹⁴ J. Bennetto, R. W. Nunes, and David Vanderbilt, *Phys. Rev. Lett* **79**, 245 (1997).
- ¹⁵ P. E. Batson, *Phys. Rev. Lett* **83**, 4409 (1999).
- ¹⁶ A. Valladares, A. K. Petford-Long, and A. P. Sutton, *Phil. Mag. Lett.* **79**, 9 (1999).
- ¹⁷ R. W. Nunes and David Vanderbilt, *Phys. Rev. Lett* **85**, 3540 (2000).

- ¹⁸ X. Blase, Karin Lin, A. Canning, S. G. Louie, and D. C. Chrzan, *Phys. Rev. Lett* **84**, 5780 (2000).
- ¹⁹ R. W. Nunes and David Vanderbilt, *J. Phys.: Condens. Matter* **12**, 10021 (2000).
- ²⁰ R. W. Nunes, J. Bennetto, and David Vanderbilt, *Phys. Rev. B* **58**, 12563 (1998).
- ²¹ Niklas Lehto and Sven Öberg, *Phys. Rev. Lett* **80**, 5568 (1998).
- ²² J. Tersoff, *Phys. Rev. B* **39**, 5566 (1989).
- ²³ H. Balamane, T. Halicioglu, and W. A. Tiller, *Phys. Rev. B* **46**, 2250 (1992).
- ²⁴ M. S. Duesbery, B. Joos, and D. J. Michel, *Phys. Rev. B* **43**, 5143 (1991).
- ²⁵ M. Z. Bazant, E. Kaxiras, and J. F. Justo, *Phys. Rev. B* **56**, 8542 (1997).
- ²⁶ J. F. Justo, M. Z. Bazant, E. Kaxiras, V. V. Bulatov, and S. Yip, *Phys. Rev. B* **58**, 2539 (1998).
- ²⁷ Caetano R. Miranda and A. Antonelli, unpublished.
- ²⁸ K. Moriguchi, S. Munetoh, A. Shintani, T. Motooka, *Phys. Rev. B* **64**, 195409 (2001).
- ²⁹ D. R. Lide and H. V. Kehiaian, *CRC Handbook of Thermophysical and Thermochemical Data*, (CRC Press, Boca Raton, 1994).
- ³⁰ D. Frenkel and B. Smit, *Understanding Molecular Simulations*, (Academic Press, San Diego, 2001).
- ³¹ Maurice de Koning, A. Antonelli, and Sidney Yip, *Phys. Rev. Lett* **83**, 3973 (1999).
- ³² Maurice de Koning and A. Antonelli *Phys. Rev. E* **53**, 465(1996); *Phys. Rev. B* **55**, 735 (1997).
- ³³ E. O. Kane, *Phys. Rev. B* **31**, 7865 (1985).
- ³⁴ G. Nilsson and G. Nelin, *Phys. Rev. B* **6**, 3777 (1972).

³⁵ The issue of supercell boundary conditions in dislocation calculations has been properly addressed in Ref. 21. When the choice of supercell vectors is such that when the cells are stacked in the direction perpendicular to the slip plane, the dislocation with Burgers vector \mathbf{b} ($-\mathbf{b}$) in one cell lies on top of the dislocation with the same Burgers vector \mathbf{b} ($-\mathbf{b}$), in the next cell, we have a dipolar configuration. On the other hand, when the cell vectors are chosen such that the dislocation with Burgers vector \mathbf{b} ($-\mathbf{b}$) lies on top of the dislocation with the opposite Burgers vector $-\mathbf{b}$ (\mathbf{b}), in the next cell, we have a quadrupolar configuration. As shown in Ref. 21, the former choice minimizes the spurious strains associated with the periodic array of dislocations, in the case of the 90° partial.

³⁶ K. Lin and D. C. Chrzan, Mater. Sci. and Eng. **A319-321**, 115 (2001).

TABLES

TABLE I. Calculated enthalpy differences at 0 K between core reconstructions of the 90° partial dislocation, for four different cell sizes, in $\text{meV}/\text{\AA}$. Results are shown for TETB (from Ref. 17), Tersoff, and EDIP. Cells are defined by their height D and width L (in \AA), as defined in the text. The number of atoms (N_{at}) in each cell is also included. ΔE_{SP} is the difference in enthalpy between the cells with the same senses and opposite senses of the SP reconstruction (see text). ΔE_{SP-DP} is the difference in enthalpy between the average of the SP cells and the DP structure.

N_{at}	L	D	Tersoff		EDIP		TBTE	
			E_{SP-DP}	ΔE_{SP}	E_{SP-DP}	ΔE_{SP}	E_{SP-DP}	ΔE_{SP}
192	13.3	18.8	13	24	-35	6	62	39
240	16.6	18.8	9	16	-39	4	55	26
576	26.6	28.2	7	6	-39	2	55	9
1920	53.2	47.0	6	2	-40	0	55	4

FIGURES

FIG. 1. Atomic structure of the 90° partial dislocation viewed from above the $\{111\}$ slip plane. (a) symmetrically reconstructed core; (b) SP reconstruction; and (c) DP reconstruction.

FIG. 2. Gibbs free-energy for the bulk of silicon. Full and dashed lines show our RS-MC calculations, including anharmonic effects, for the EDIP and Tersoff potentials, respectively. The dotted line shows the Tersoff-potential harmonic-approximation results from Ref. 28, and the squares are the experimental results from Ref. 29.

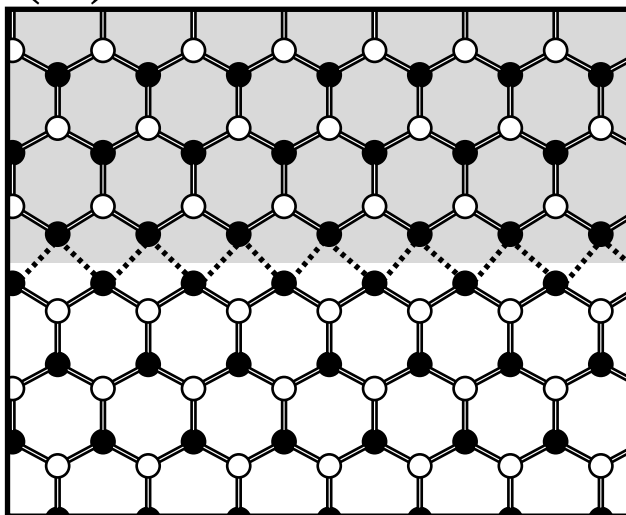
FIG. 3. Gibbs free-energy difference per unit length ΔG , between the SP and the DP geometries of the 90° partial dislocation in silicon, with different samplings of the phonon modes along the dislocation direction. For the 192-atom calculations, the results for the SP cores with same reconstruction senses, with opposite reconstruction senses, and the average between the two (as explained in the text) are shown by the squares, circles, and triangles, respectively. For the 384-atom cell, same reconstruction senses, opposite reconstruction senses, and the average are represented by the solid line, the dashed line, and the dotted line, respectively.

FIG. 4. Gibbs free-energy difference per unit length (ΔG) and the entropic contribution $-T\Delta S$, between the SP and the DP geometries in silicon, in $\text{meV}/\text{\AA}$, using the Tersoff potential (full line for ΔG and squares for $-T\Delta S$), and the EDIP potential (dashed line for ΔG and circles for $-T\Delta S$).

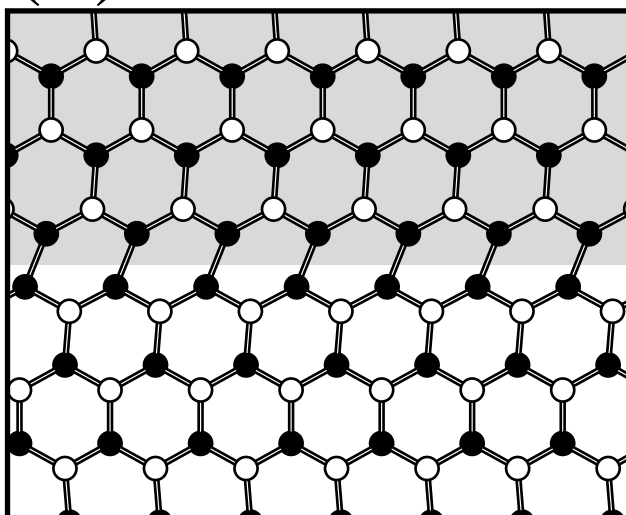
FIG. 5. Gibbs free-energy difference per unit length ΔG , and the entropic contribution $-T\Delta S$, in $\text{meV}/\text{\AA}$, between the SP and the DP geometries in germanium, using the Tersoff potential (full line for ΔG and squares for $-T\Delta S$).

FIG. 6. Difference in free energy between SP and DP cores in silicon for RS-MC calculations using the Tersoff (full line) and EDIP (dashed line) potentials, compared with the harmonic-approximation results from Ref. 10. RS-MC energies at 0 K were shifted, for better comparison (see text).

(a)



(b)



(c)

